DESIGN OF THE ECMWF NORMAL MODE INITIALIZATION PROCEDURE

C. Temperton
ECMWF*

*Present affiliation: UK Meteorological Office, Bracknell

1. NORMAL MODE INITIALIZATION FOR THE ECMWF GRIDPOINT MODEL

1.1 Introduction

During the early stages of the development of the ECMWF data assimilation system, it was envisaged that a systematic program of research would be required to determine which of the various available initialization techniques would be most appropriate for inclusion in the assimilation cycle. The first technique to be tried was normal mode initialization, which at that time had only been applied to barotropic models (Williamson, 1976), though the basis had already been laid for its application to multi-level models (Dickinson and Williamson, 1972; Williamson and Dickinson 1976). The extension by Machenhauer (1977) to include nonlinear forcing had been highly effective when applied to a barotropic spectral model, and it was this result which provided the incentive to try Machenhauer's technique in a multi-level gridpoint model. The attempt proved so successful that, apart from an experiment to confirm the great superiority of nonlinear normal mode initialization over dynamic initialization (previously considered to be another promising candidate), no further work was done on other initialization techniques.

Normal mode initialization methods are based on the normal mode solutions of the forecast model, linearized about a stationary basic state. The solutions can be classified, in terms of their frequencies, into Rossby modes (low frequency) and inertia-gravity modes (high frequency). Only the former are observed with significant amplitude in the real atmosphere, and the purpose of initialization techniques is essentially to provide initial conditions such that the same is true of the numerical model atmosphere during a subsequent integration.

In Section 1.2 of this paper we derive the normal modes of the ECMWF multi-level gridpoint model. In Section 1.3 we apply linear normal mode initialization, and show that it is not very successful. In Section 1.4 we demonstrate the success of Machenhauer's nonlinear normal mode initialization technique applied to the model. Section 2 outlines some extensions and variations of the procedure.

1.2 Determination of the normal modes

To keep the determination of the normal modes computationally practicable, we require that the linearized equations be separable. We therefore choose a simple basic state at rest, with temperature $\bar{T}(\sigma)$ varying only as a function of σ, and constant surface pressure $\bar{p}_s$. (This implies that the model mountains are not included in the basic state). For the moment we discretize only in the vertical. The linearized perturbation equations are then:

$$\frac{\partial u_n}{\partial t} - fv_n + \frac{1}{a\cos\theta}\frac{\partial}{\partial\lambda}\bar{\phi}^{\sigma}_n + \frac{R\bar{T}_n}{a\cos\theta}\frac{\partial}{\partial\lambda}(\ell n\ p_s) = o \tag{1}$$

$$\frac{\partial v_n}{\partial t} + fu_n + \frac{1}{a}\frac{\partial}{\partial\theta}\bar{\phi}^{\sigma}_n + \frac{R\bar{T}_n}{a}\frac{\partial}{\partial\theta}(\ell n\ p_s) = o \tag{2}$$

$$\frac{\partial T_n}{\partial t} - \frac{\kappa\bar{T}_n}{\sigma_n}\left(\sigma\frac{\partial(\ell n\ p_s)}{\partial t} + \dot{\sigma}\right)^{\sigma}_n + \left(\dot{\sigma}\,\delta_{\sigma}\,\bar{T}\right)^{\sigma}_n = o \tag{3}$$

$$\frac{\partial(\ell n\ p_s)}{\partial t} + \sum_{\ell=1}^{N}\chi_{\ell}(\Delta\sigma)_{\ell} = o \tag{4}$$

where χ is divergence, and other symbols have their usual meanings. The hydrostatic equation is

$$\phi_{n+\frac{1}{2}} = \phi_s + \sum_{\ell=n+1}^{N} RT_{\ell}\,(\Delta\ \ell n\sigma)_{\ell} \tag{5}$$

and the linearized diagnostic equation for the vertical velocity $\dot{\sigma}$ is

$$\dot{\sigma}_{n+\frac{1}{2}} = \sigma_{n+\frac{1}{2}}\sum_{\ell=1}^{N}\chi_{\ell}(\Delta\sigma)_{\ell} - \sum_{\ell=1}^{n}\chi_{\ell}\,(\Delta\sigma)_{\ell} \tag{6}$$

We define an auxiliary variable h_n by

$$gh_n = \bar{\phi}^{\sigma}_n + R\bar{T}_n\ \ell n\ p_s \tag{7}$$

and a column vector by $\underset{\sim}{u} = (u_1, u_2, \ldots, u_N)^T$, and similarly for $\underset{\sim}{v}$, $\underset{\sim}{h}$, $\underset{\sim}{\chi}$, $\underset{\sim}{T}$, $\underset{\sim}{\phi}$.

Using (6) and (7), we can rewrite Equations (1) to (5) in the form:

$$\frac{\partial \underset{\sim}{u}}{\partial t} - f\underset{\sim}{v} + \frac{g}{a\cos\theta}\frac{\partial \underset{\sim}{h}}{\partial \lambda} = \underset{\sim}{o} \tag{8}$$

$$\frac{\partial \underset{\sim}{v}}{\partial t} + f\underset{\sim}{u} + \frac{g}{a}\frac{\partial \underset{\sim}{h}}{\partial \theta} = \underset{\sim}{o} \tag{9}$$

$$\frac{\partial \underset{\sim}{T}}{\partial t} + \tau\underset{\sim}{\chi} = \underset{\sim}{o} \tag{10}$$

$$\frac{\partial(\ell n p_s)}{\partial t} + \Pi^T \underset{\sim}{\chi} = \underset{\sim}{o} \tag{11}$$

$$\underset{\sim}{\phi} = \underset{\sim}{\phi}_s + G\underset{\sim}{T} \tag{12}$$

Details of the matrices τ, G, Π^T are given in Temperton and Williamson (1979). Finally we can combine (10) - (12) to give

$$g\frac{\partial \underset{\sim}{h}}{\partial t} + C\underset{\sim}{\chi} = \underset{\sim}{o} \tag{13}$$

where

$$C = G\tau + R\underset{\sim}{\bar{T}}\,\Pi^T \tag{14}$$

In order to separate variables and determine the vertical structure of the normal modes, we use the eigenvalues of C, denoted by gD_m, and the corresponding eigenvectors $\underset{\sim}{\Phi}_m$. Let B be the matrix whose columns are the eigenvectors of C, and let gD be the diagonal matrix of corresponding eigenvalues. Then

$$C = g\,B\,D\,B^{-1} \tag{15}$$

and the vertical transformation

$$\underset{\sim}{\bar{u}} = B^{-1}\underset{\sim}{u},\ \underset{\sim}{\bar{v}} = B^{-1}\underset{\sim}{v},\ \underset{\sim}{\bar{h}} = B^{-1}\underset{\sim}{h},\ \underset{\sim}{\bar{\chi}} = B^{-1}\underset{\sim}{\chi} \tag{16}$$

gives

$$\frac{\partial \underset{\sim}{\bar{u}}}{\partial t} - f\underset{\sim}{\bar{v}} + \frac{g}{a\cos\theta}\frac{\partial \underset{\sim}{\bar{h}}}{\partial \lambda} = \underset{\sim}{o} \tag{17}$$

$$\frac{\partial \underset{\sim}{\bar{v}}}{\partial t} + f\underset{\sim}{\bar{u}} + \frac{g}{a}\frac{\partial \underset{\sim}{\bar{h}}}{\partial \theta} = \underset{\sim}{o} \tag{18}$$

$$\frac{\partial \underset{\sim}{\bar{h}}}{\partial t} + D\,\underset{\sim}{\bar{\chi}} = \underset{\sim}{o} \tag{19}$$

Since D is diagonal, (17) - (19) represents an uncoupled system of equations for the coefficients of each vertical mode:

$$\frac{\partial \bar{u}_m}{\partial t} - f\bar{v}_m + \frac{g}{a\cos\theta}\frac{\partial \bar{h}_m}{\partial \lambda} = o \qquad (20)$$

$$\frac{\partial \bar{v}_m}{\partial t} + f\bar{u}_m + \frac{g}{a}\frac{\partial \bar{h}_m}{\partial \theta} = o \qquad (21)$$

$$\frac{\partial \bar{h}_m}{\partial t} + D_m \bar{\chi}_m = o \qquad (22)$$

Thus the coefficients of the mth vertical mode satisfy the shallow water equations with mean depth D_m. Table 1 lists the equivalent depths for the vertical modes of a 9-level version of the ECMWF model, using global means from a particular analysis to define the basic vertical temperature profile $\bar{T}(\sigma)$. Also listed are the corresponding phase speeds of the gravity waves on a non-rotating earth, $\sqrt{gD_m}$. The corresponding eigenvectors (vertical normal modes) are shown in Fig. 1. The first eigenvector (the external mode), with the largest equivalent depth, has the same sign throughout. Each successive internal mode has one additional sign change until the last internal mode, with the smallest equivalent depth, which changes sign between each model level. The vertical modes are orthogonal only if the basic temperature profile $\bar{T}(\sigma)$ is isothermal.

For each vertical mode, we can now determine the corresponding horizontal normal modes. The longitudinal dependence of the variables in (20) - (22) is separated out simply by Fourier transforming the equations. Setting

$$\bar{u}(\lambda_i, \theta_j, m) = \sum_{k=o}^{N-1} \tilde{u}(k, \theta_j, m) \exp(ik\lambda_i) \qquad (23)$$

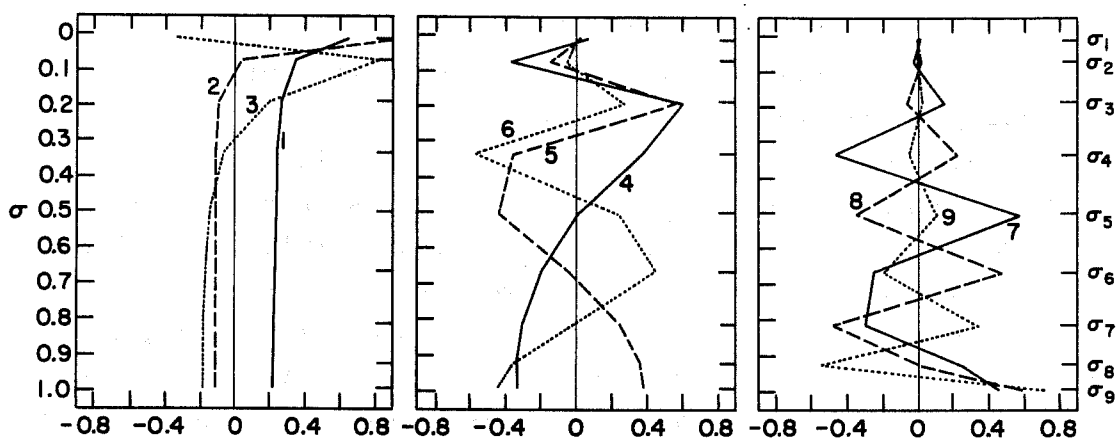

Fig. 1 Vertical normal modes of 9-level model, $\bar{T}(\sigma)$ from analysis of 1st March 1965.

Table 1. Equivalent depths (m) and corresponding gravity wave phase speeds (ms^{-1}) of vertical normal modes, 9-level model

Vertical mode index m	depth (D_m)	phase speed ($\sqrt{gD_m}$)
1	10153	315.4
2	4701	214.6
3	851	91.3
4	205	44.8
5	65	25.2
6	20	14.0
7	7.3	8.4
8	2.4	4.8
9	0.5	2.2

and similarly for the other variables, we obtain equations of the form:

$$\frac{\partial \tilde{u}_j}{\partial t} - [\tilde{fv}]_j + g \frac{ik'}{a\cos\theta_j} \tilde{h}_j = o \tag{24}$$

$$\frac{\partial \tilde{v}_{j+\frac{1}{2}}}{\partial t} + [\tilde{fu}]_{j+\frac{1}{2}} + \frac{g}{a} (\delta_\theta \tilde{h})_{j+\frac{1}{2}} = o \tag{25}$$

$$\frac{\partial \tilde{h}_j}{\partial t} + \frac{D_m}{a\cos\theta_j} \{ik' \tilde{u}_j + (\delta_\theta(\tilde{v}\cos\theta))_j\} = o \tag{26}$$

where, to simplify the notation, we have dropped the vertical mode index m and the Fourier wavenumber k from the variables. The longitudinal differencing is taken account of by defining

$$k' = (\sin \tfrac{1}{2} k\Delta\lambda)/(\tfrac{1}{2} \Delta\lambda) \tag{27}$$

The details of the Coriolis terms $[\tilde{fv}]_j$ and $[\tilde{fu}]_{j+\frac{1}{2}}$ are given in Temperton and Williamson (1979).

Equations (24) - (26) represent a set of coupled simultaneous equations for u_j, $v_{j+\frac{1}{2}}$, h_j as j runs from pole to pole. The only possible further separation is to write u_j, $v_{j+\frac{1}{2}}$, h_j as the sum of two components, respectively symmetric and antisymmetric about the equator. We can then solve two smaller sets of simultaneous equations in which j runs from pole to equator, one for "symmetric" components ($\tilde{u}$, $\tilde{h}$ symmetric, $\tilde{v}$ antisymmetric), and similarly for "antisymmetric" components.

Using the transformation

$$\hat{u}_j = \tilde{u}_j \ , \ \hat{v}_{j+\frac{1}{2}} = - i\tilde{v}_{j+\frac{1}{2}} \ , \ \hat{h}_j = (g/D_m)^{\frac{1}{2}} \tilde{h}_j \tag{28}$$

and defining

$$\underset{\sim}{Y} = (\hat{u}_1, \hat{h}_1, \hat{v}_{1\frac{1}{2}} , \ldots\ldots, \hat{u}_j, \hat{h}_j, \hat{v}_{j+\frac{1}{2}}, \ldots) \tag{29}$$

which represents a vector of variables defined from pole to equator, (24) - (26) can now be written in the form:

$$Q \frac{\partial \underset{\sim}{Y}}{\partial t} - iL\underset{\sim}{Y} = \underset{\sim}{o} \tag{30}$$

where Q is diagonal (and positive) and L is symmetric. To recast (30) in standard form, define

$$\hat{\underset{\sim}{Y}} = Q^{\frac{1}{2}} \underset{\sim}{Y} \ , \ \hat{L} = Q^{-\frac{1}{2}} L Q^{-\frac{1}{2}} \tag{31}$$

so that

$$\frac{\partial \hat{\underset{\sim}{Y}}}{\partial t} - i\hat{L}\hat{\underset{\sim}{Y}} = \underset{\sim}{o} \tag{32}$$

(Reminder: we have an equation of the form (32) for each vertical mode m, each Fourier wavenumber k, and each of the two symmetry conditions).

To determine the normal modes of (32), let E be the matrix whose columns ψ_ℓ are eigenvectors of $\hat{L}$, and let Λ be the diagonal matrix of corresponding eigenvalues ν_ℓ'. Since L was symmetric, so is $\hat{L}$, and hence (32) becomes

$$\frac{\partial \underset{\sim}{c}}{\partial t} - i\Lambda \underset{\sim}{c} = \underset{\sim}{o} \qquad (33)$$

where

$$\underset{\sim}{c} = E^T \hat{\underset{\sim}{Y}} = E^T Q^{\frac{1}{2}} \underset{\sim}{Y} \qquad (34)$$

Since Λ is diagonal, (33) is a set of uncoupled equations of the form

$$\frac{\partial c_\ell}{\partial t} - i\nu'_\ell \, c_\ell = o \qquad (35)$$

Each c_ℓ is the coefficient of the corresponding normal mode $\underset{\sim}{\psi}_\ell$, and (35) is a linear equation for its evolution in time, with solution

$$c_\ell (t) = c_\ell (o) \exp (i\nu'_\ell \, t) \qquad (36)$$

Each normal mode $\underset{\sim}{\psi}_\ell$ has a characteristic meridional structure given by its components (u,v,h). For each matrix E, the modes can be classified into three groups, according to their frequencies ν'_ℓ : the low-frequency westward propagating Rossby modes and the high-frequency eastward and westward propagating gravity modes. The modes within each group can be indexed in terms of their frequency ordering. For the larger equivalent depths there is a close correspondence between the indexing and the number of zero crossings of each variable between the poles, just as in the continuous case (Longuet-Higgins, 1968). The magnitudes of the frequencies of the gravity modes increase with increasing index, while those of the Rossby modes decrease. For the smaller equivalent depths (high internal modes), the horizontal modes resemble the continuous modes less closely, tending to be more of a computational nature.

The model equations may be modified by Fourier filtering or chopping the time-tendencies of the variables in order to increase the maximum stable timestep (Burridge and Haseler, 1977). This modification can be included in the normal mode analysis by modifying the matrix Q in (30); the details are given in Temperton (1977).

1.3 Linear normal mode initialization

In linear normal mode initialization, the initial data is first expanded into normal modes, the coefficients of the unwanted gravity modes are set to zero, and a modified set of initial data is reconstructed from the remaining modes. The expansion is done sequentially following the analysis of Section 1.2. The basic state is first subtracted from the prognostic variables, then a field of the auxiliary variable h is constructed using (7). The data are expanded into vertical modes using (16), and each vertical mode is expanded into Fourier modes using the inverse of (23). The symmetric and antisymmetric components are found by averaging or differencing the values from the two hemispheres, and scaled using (28). Finally, each scaled Fourier mode of each vertical mode is expanded into latitudinal modes by (34).

Those coefficients corresponding to unwanted modes can then be set to zero, and the expansion procedure reversed to obtain a new set of gridpoint data. For the multi-level σ-coordinate model, there is one remaining problem: we have obtained a new field of the auxiliary variable h, which then has to be decomposed into new fields of p_s and $\bar{\phi}^{\sigma}$(and hence T). As shown by Andersen (1977) and Temperton and Williamson (1979), the correct procedure is to define the change in $\ell n\ (p_s)$ by

$$\Delta \ell n\ (p_s) = \Pi^T\ C^{-1}\ g\ \underset{\sim}{\Delta h} \qquad (37)$$

Given new fields of p_s and h, the new temperature field can easily be computed.

The question remains as to whether it is necessary to initialize all the model's gravity mode coefficients in this way. We saw in Section 1.2 that the frequencies of the highest internal gravity modes (with the smallest equivalent depths) are so low that they do not contribute to the problem of spurious high-frequency oscillations. It is convenient to zero all the gravity mode coefficients for the first m vertical modes, and in practice m=5 has been found a suitable choice.

In this section and the next, we describe initialization experiments using a 9-level global model with a horizontal resolution of $\Delta\lambda = \Delta\theta = 3.75^{o}$ (N24). The initial data consisted of global fields

of temperature, wind and surface pressure for 00Z on 1 March 1965, as analysed at GFDL and subsequently interpolated to the ECMWF model grid. The results of each initialization experiment were used as initial data for a 24-hour adiabatic forecast. At each timestep, the values of selected variables at four horizontal gridpoints were written to a history file. Time-filtering and horizontal diffusion were switched off, in order to show up any high-frequency oscillations in the forecasts.

Fig. 2 shows the evolution of surface pressure at two gridpoints for the two 24-hour forecasts, one from the original data, and one from a linear initialization experiment in which the gravity mode coefficients were set to zero for the first 5 vertical modes. The forecast from the original data is severely contaminated by high-frequency oscillations, implying a poor state of balance in the initial conditions. As in the shallow-water experiments of Williamson (1976), linear normal mode initialization reduces the amplitude of the oscillations, but by no means eliminates them.

Two factors contribute towards this result. Firstly, the high-frequency gravity modes, although absent from the initial data, are rapidly regenerated in the model through nonlinear interactions. Secondly, the initialization is very poor over mountains. As pointed out in Section 1.2, the basic state is defined assuming no topography. Consequently, over high topography there will be large deviations from the basic state, and these will be misinterpreted as gravity waves, removal of which requires large adjustments to the mass field. Fortunately, as we shall see in Section 1.4, this problem is solved by extending the normal mode initialization procedure to include nonlinear forcing.

1.4 Nonlinear normal mode initialization

As we saw in Section 1.3, the device of setting to zero the initial values of the gravity mode coefficients does not prevent these modes from oscillating, because of forcing by the model's nonlinear terms. Machenhauer (1977) proposed a nonlinear correction technique in which the initial time tendencies of the gravity mode coefficients are set to zero, rather than the coefficients themselves.

If the nonlinear terms are included, Eq. (35) becomes

$$\frac{\partial c_\ell}{\partial t} - i\nu'_\ell c_\ell = r_\ell \tag{38}$$

where r_ℓ represents the nonlinear contribution to the tendency of the coefficient c_ℓ. The basis of Machenhauer's technique is the assumption that r_ℓ varies much more slowly than the linear frequency of the modes being modified, and can thus be treated as a constant. In this case the solution of (38) is

$$c_\ell(t) = \frac{r_\ell}{i\nu'_\ell} + [c_\ell(o) - \frac{r_\ell}{i\nu'_\ell}] \exp(i\nu'_\ell t) \tag{39}$$

If we set $c_\ell(o) = r_\ell/i\nu'_\ell$, then the oscillatory term in (39) vanishes and the coefficient c_ℓ becomes independent of time. Since the nonlinear terms are not constant, and in fact depend partly on the initial values of the mode coefficients themselves, Machenhauer proposed the following iterative procedure to zero the initial time tendencies of the gravity mode coefficients:

$$[c_\ell(o)]_{\mu+1} = [r_\ell(o)]_\mu / i\nu'_\ell \tag{40}$$

where $[r_\ell(o)]_\mu$ is computed from the nonlinear terms using initial conditions from $[c_\ell(o)]_\mu$. The simplest way to implement (40) is just to run the model for one forward timestep: Eq. (38) then becomes

$$[c_\ell(\Delta t)]_\mu - [c_\ell(o)]_\mu = i\nu'_\ell \Delta t [c_\ell(o)]_\mu + r_\ell(o) \Delta t \tag{41}$$

and hence, by substituting in (40),

$$[c_\ell(o)]_{\mu+1} = [c_\ell(o)]_\mu + \frac{[c_\ell(\Delta t)]_\mu - [c_\ell(o)]_\mu}{i\nu'_\ell \Delta t} \tag{42}$$

Eq. (42) contains no explicit reference to the nonlinear terms, so there is no need to modify the model code to extract them. Note that the timestep length Δt in (42) cancels out with the forward difference, so the iterative procedure is independent of the choice of Δt.

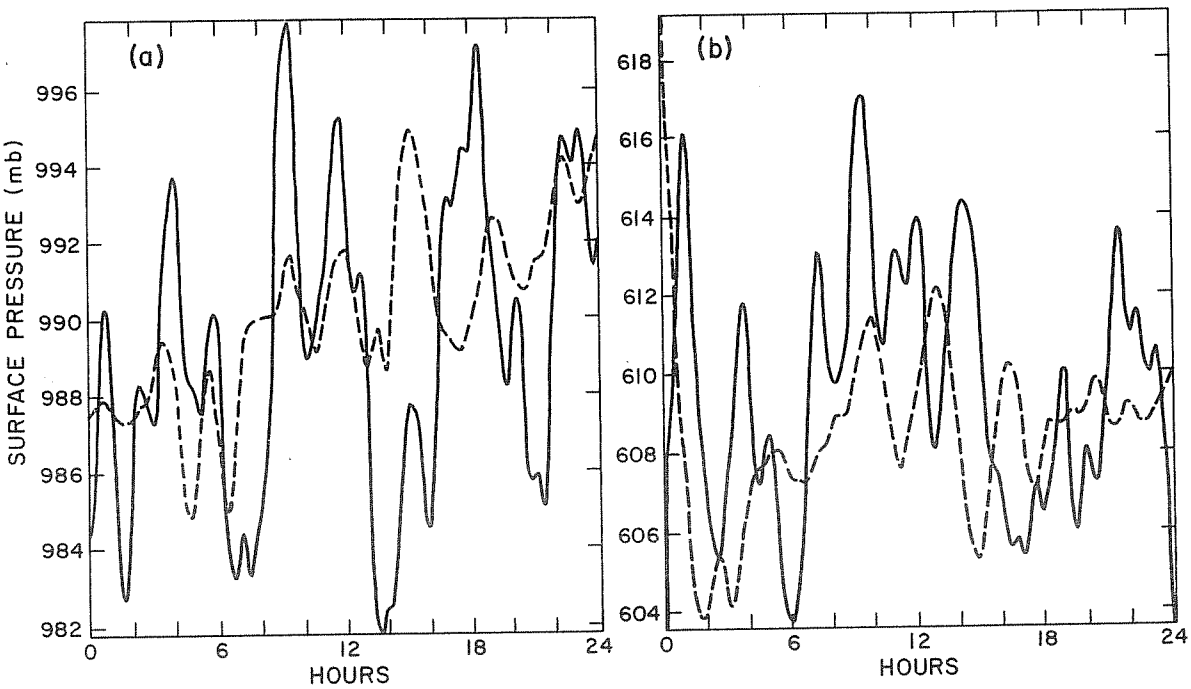

Fig. 2 Surface pressure vs. time before (____) and after (---) linear normal mode initialization: (a) 40°N, 90°W; (b) 30°N, 90°E.

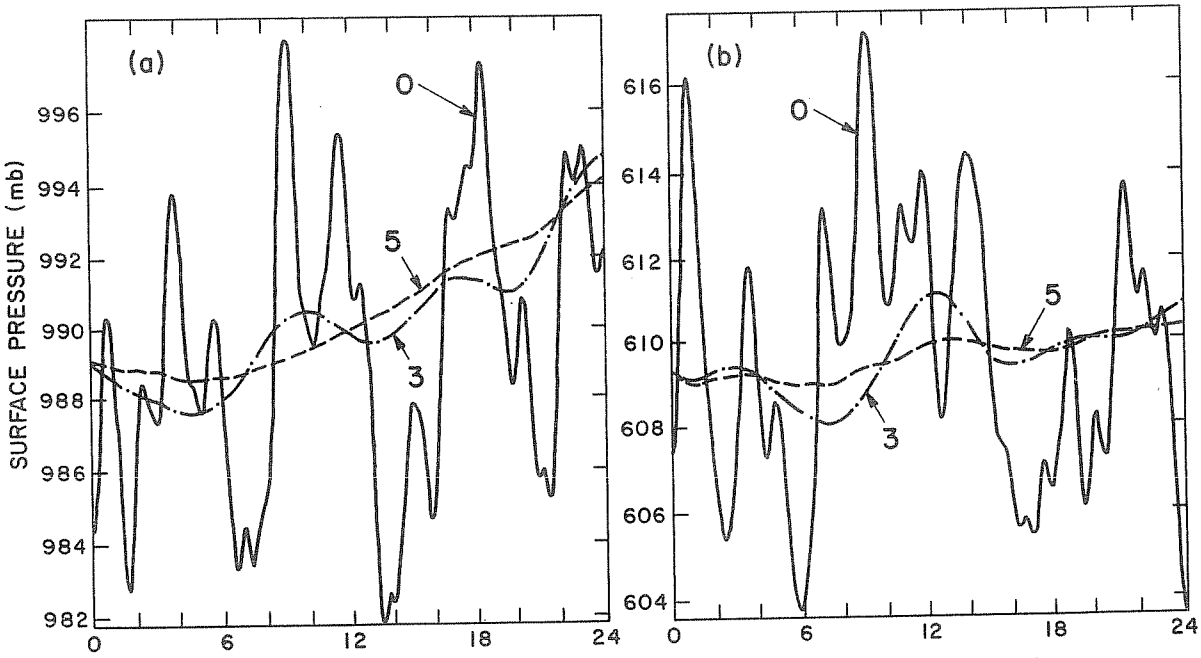

Fig. 3 Surface pressure vs. time at (a) 40°N, 90°W, (b) 30°N, 90°E after non-linear normal mode initialization of 0, 3 and 5 vertical modes.

Fig. 3 shows the evolution of surface pressure during 24-hour adiabatic forecasts from the same initial data as before, after applying 2 iterations of Machenhauer's nonlinear normal mode initialization technique to the first 3 and 5 vertical modes, compared with the same forecast from uninitialized data (o vertical modes). Initialization of 5 vertical modes virtually eliminates all high-frequency oscillations, leaving variations only on synoptic time-scales.

This highly successful result was obtained after only two iterations of the procedure; is even the second iteration necessary? Fig. 4 compares results after one and two iterations (note that the scale is greatly expanded). Most of the improvement comes from the first iteration, but the second does provide additional improvement.

We have not yet examined the question of convergence of the iterative procedure. As we are trying to force the initial time tendencies of the gravity modes to zero, a convenient quantity to monitor (Andersen, 1977) is

$$BAL_m = \sum_{\ell} \left[\frac{\partial c_{\ell}(o)}{\partial t}\right]^2 \qquad (43)$$

where the sum is taken over all the gravity modes being initialized, for vertical mode m. Fig. 5 shows this quantity for vertical modes $1 \leqslant m \leqslant 5$ during 4 iterations. Little reduction occurs after the first two iterations - i.e., BAL_m does not actually converge to zero - but by this time the gravity mode time tendencies have been reduced by several orders of magnitude.

A further question concerns the influence of the choice of basic vertical temperature profile $\bar{T}(\sigma)$; in the experiments described so far $\bar{T}(\sigma)$ was taken from the data being initialized. Fig. 6 compares these results with an experiment in which a warm isothermal atmosphere was used as the basic state, $\bar{T}(\sigma) = 300^{o}K$. Very little deterioration results from using this quite unrealistic basic state, and in most subsequent work an approximate ICAO standard atmosphere has been used to provide the basic profile.

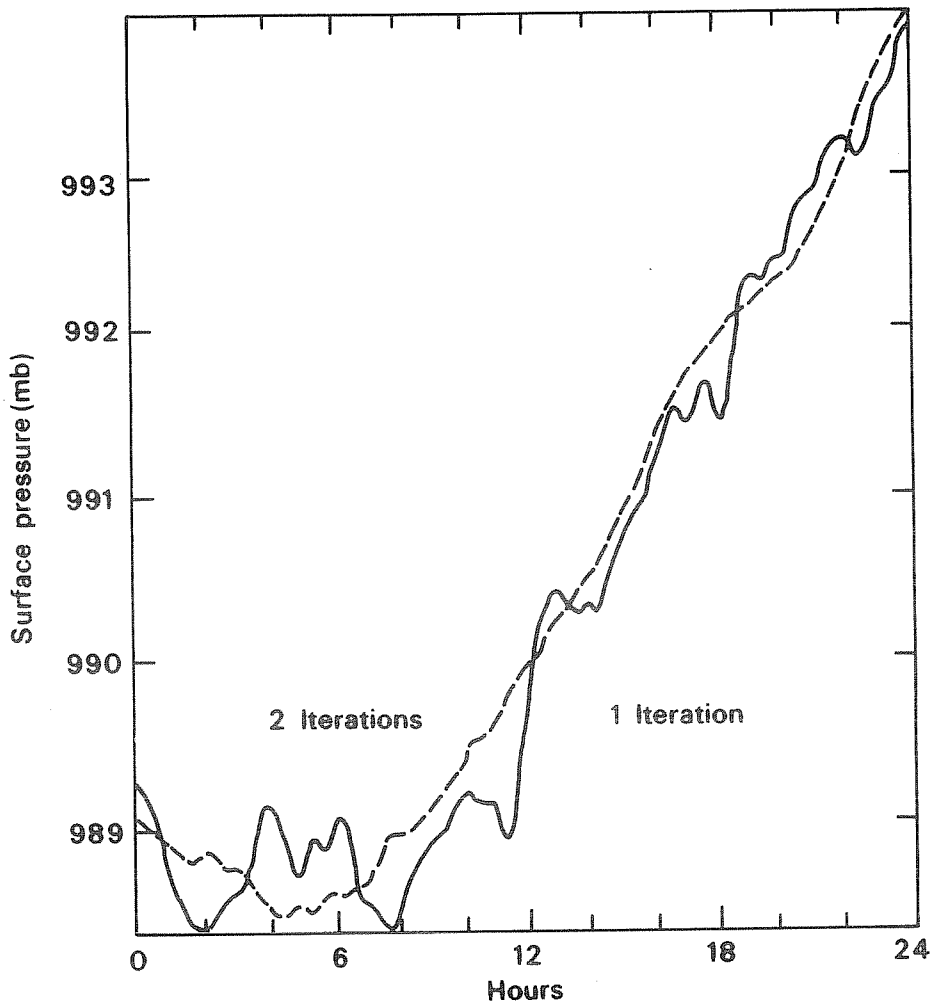

Fig. 4 Surface pressure vs. time at 40°N, 90°W after 1 and 2 iterations of nonlinear normal mode initialization (5 vertical modes).

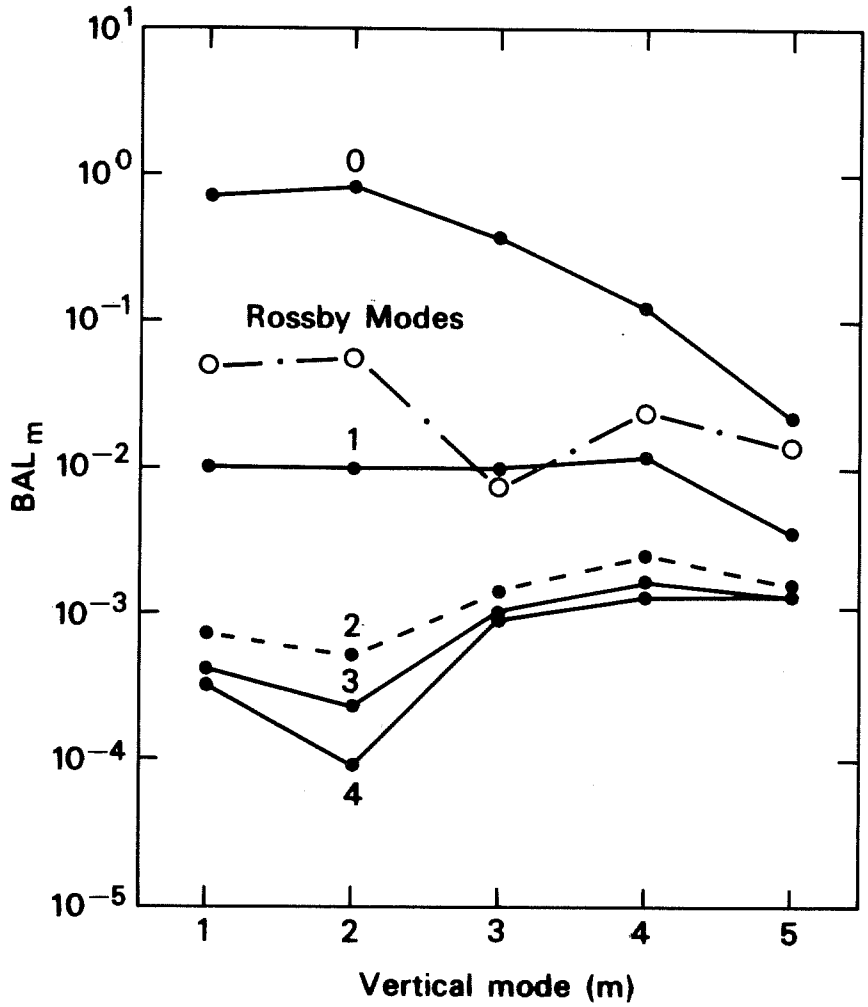

Fig. 5 "Balance" of symmetric gravity modes after each nonlinear iteration on the first 5 vertical modes.

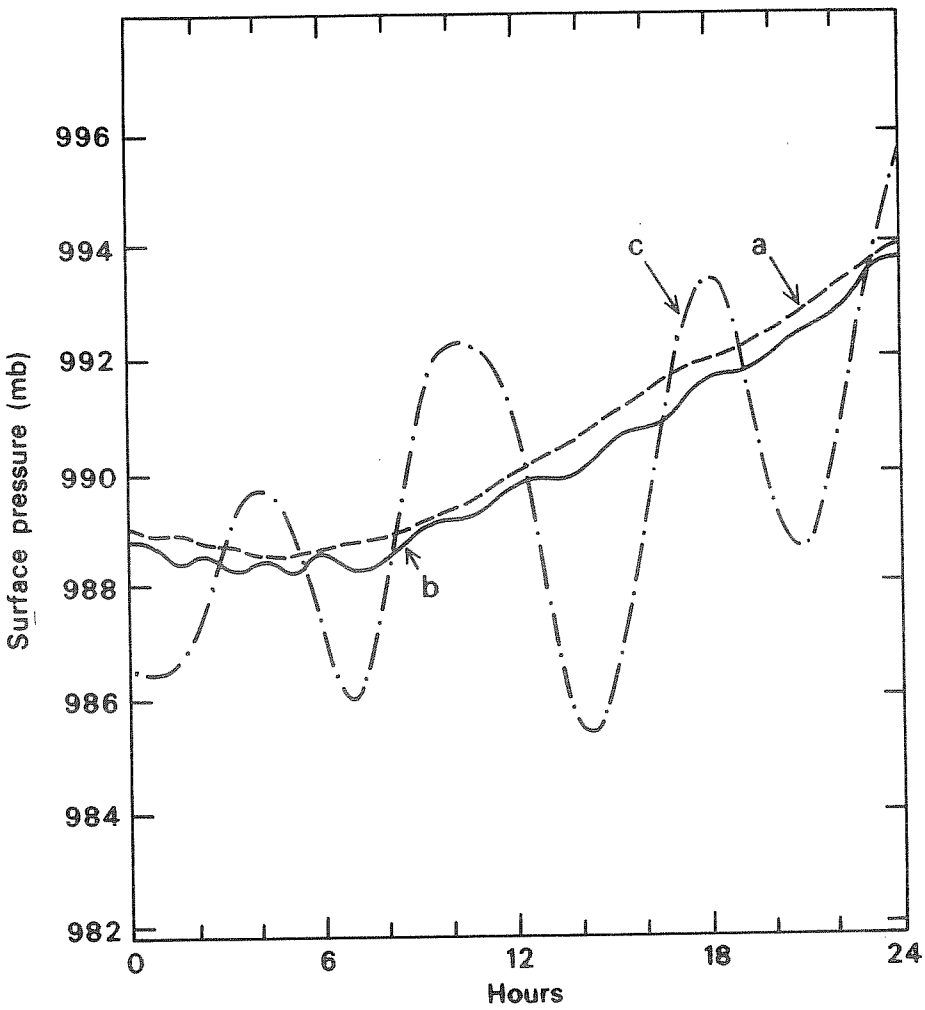

Fig. 6 Surface pressure vs. time after

(a) 2 nonlinear iterations, 5 vertical modes, $\bar{T}(\sigma)$ from analysis;

(b) 2 nonlinear iterations, 5 vertical modes, $\bar{T}(\sigma) \equiv 300^{o}K$

(c) 6 hours of dynamic initialization

Also shown in Fig. 6 is the evolution of surface pressure after 6 hours of dynamic initialization, using the scheme due to Okamura (Nitta, 1969). As expected, the highest frequencies are eliminated, but substantial oscillations remain with periods of the order of eight hours. It is clear that dynamic initialization is much less successful than nonlinear normal mode initialization - and yet 6 hours of dynamic initialization takes about 40 times as much computer time as each iteration of nonlinear normal mode initialization!

2. EXTENSIONS AND VARIATIONS OF THE ECMWF NORMAL MODE INITIALIZATION PROCEDURE

2.1 Inclusion of physics

In Section 1 we demonstrated the success of Machenhauer's (1977) nonlinear iterative technique in initializing an adiabatic version of the forecast model. In practice, of course, the model includes a wide variety of parameterizations of sub-gridscale physical processes, all of which contribute to the nonlinear term r_ℓ in Eq. (38), and thereby alter the balance which the initialization procedure is seeking to obtain. The simplest example is perhaps the modification of geostrophic balance by friction in the boundary layer. In fact boundary layer processes are not a serious problem, at least in the context of data assimilation; examination of the structure of the vertical modes (Fig. 1) shows that such processes will be described mainly by the highest internal modes (with small equivalent depths and correspondingly low frequencies), which are not initialized anyway. If the original data has consistently balanced fields in the boundary layer (for example generated by the model in providing the first-guess field, and preserved by the analysis scheme), then this balance will not be destroyed by an adiabatic initialization of the external and first few internal modes of the model.

A more serious problem concerns those processes which operate through a considerable depth of the atmosphere, for example convection and latent heat release. Concern has been expressed at the treatment of the mean meridional circulation, in particular the equatorial Hadley cell, by the adiabatic initialization procedure. Figs. 7 and 8 show the mean meridional circulation in the first-guess field and subsequent analysis during a particular data assimilation experiment; note that the strength of the Hadley cell has been well preserved in the analysis. Fig. 9 shows the corresponding circulation after the standard initialization scheme; the Hadley cell has been almost obliterated, since the adiabatic initialization procedure can see no reason for maintaining it. (Note, incidentally, that the mean meridional circulation consists entirely of gravity modes, since the Rossby modes for zonal mean flow are characterized by $v = o$).

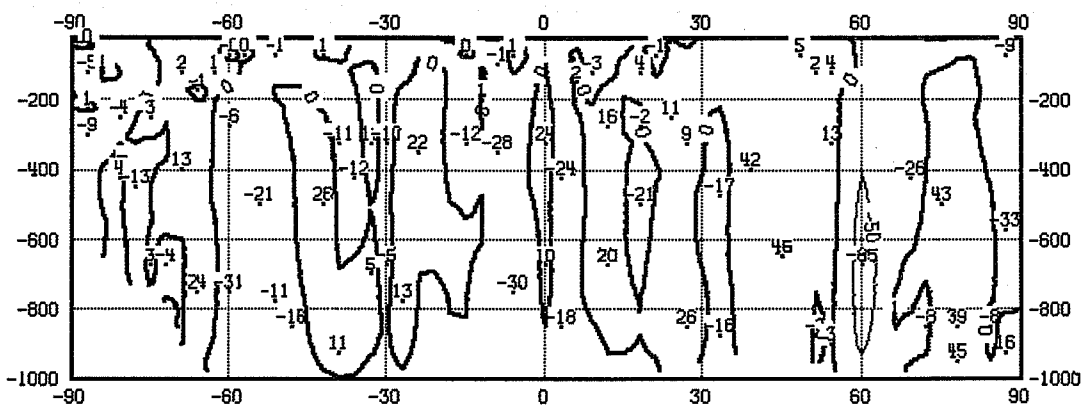

MEAN VERT WIND (DP/DT MPA/S)
1979/ 1/15 18Z FCQ1PA FIRST-GUESS

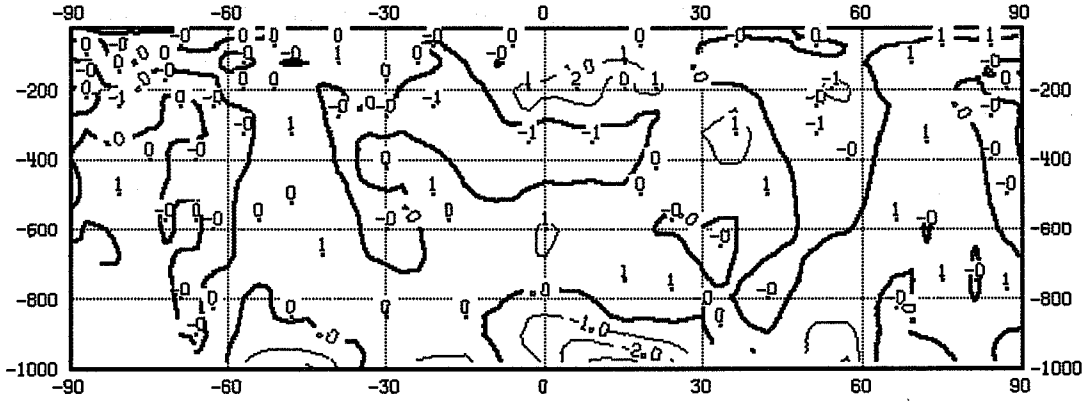

MEAN V-WIND (M/S)
1979/ 1/15 18Z FCQ1PA FIRST-GUESS

Fig. 7 Mean meridional circulation, first-guess field.

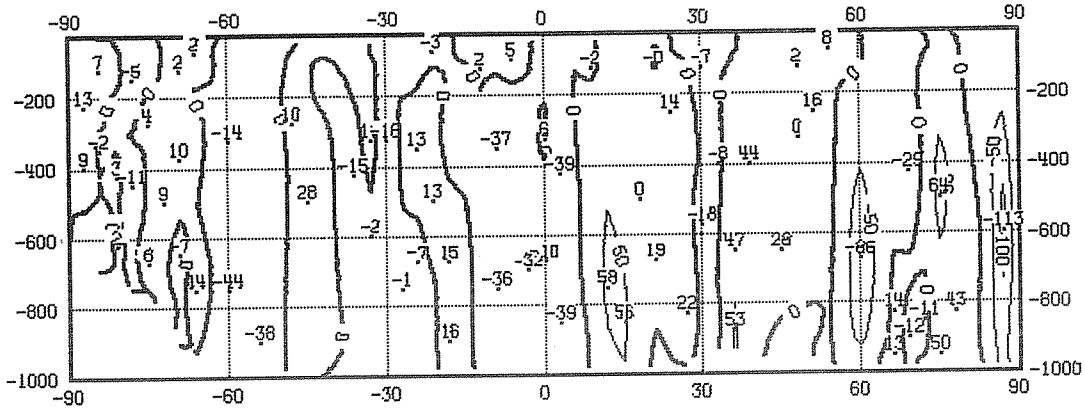

MEAN VERT WIND (DP/DT MPA/S)
1979/ 1/16 0Z SNQ1PA ANALYSIS

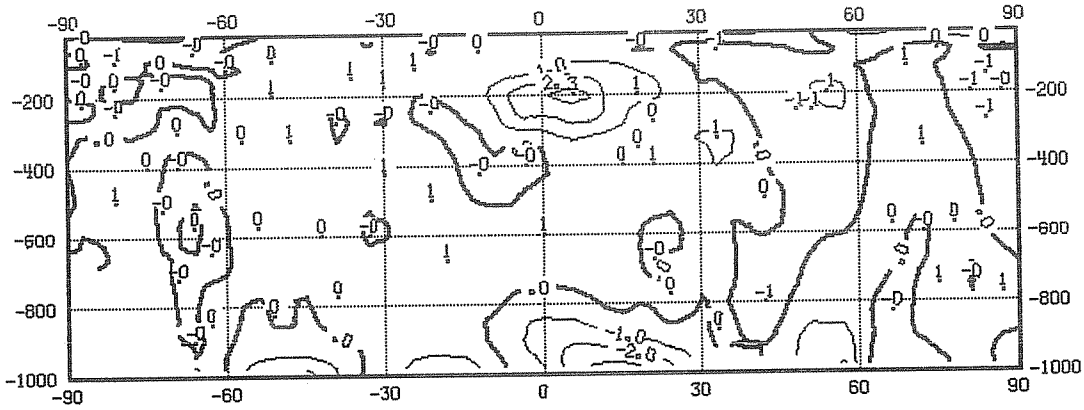

MEAN V-WIND (M/S)
1979/ 1/16 0Z SNQ1PA ANALYSIS

Fig. 8 Mean meridional circulation, analysis.

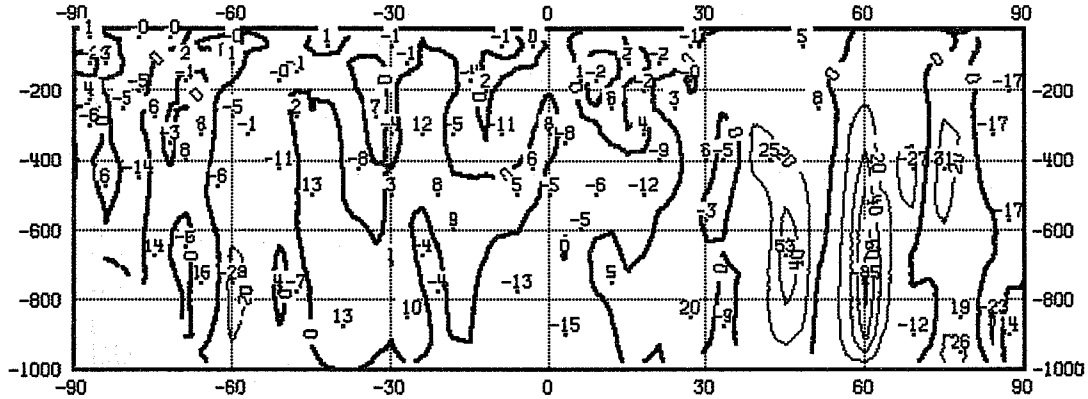

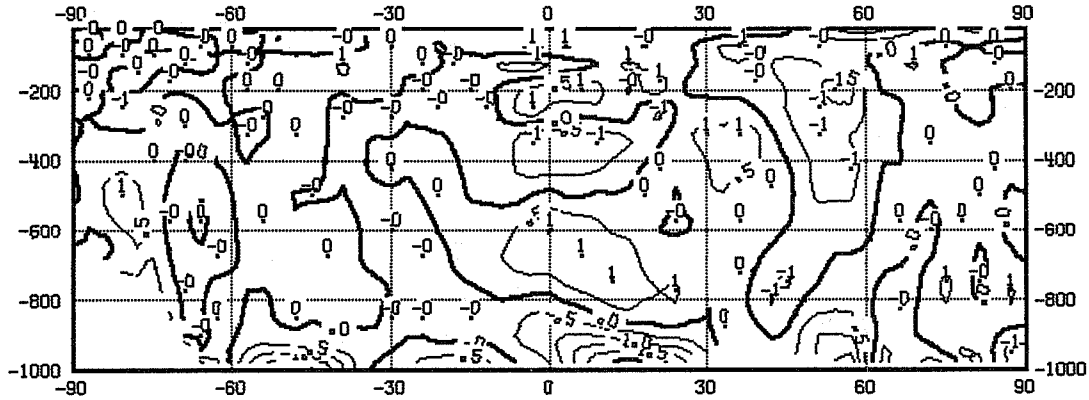

Fig. 9 Mean meridional circulation after standard initialization.

In principle there seems to be no reason why the contribution of physical processes to the nonlinear forcing should not be included in the term $r_{\ell}(o)$ in Eq. (40); indeed, this feature at first appeared to be a further advantage of nonlinear normal mode initialization over other techniques. Unfortunately, this is the one aspect of the procedure which has not lived up to its original promise. When the physical processes are included in the nonlinear forcing, the initialization procedure tends to diverge rather rapidly. Presumably this results from violation of the assumption that the nonlinear forcing changes only slowly compared with the linear frequencies of the modes, and/or excessive nonlinearity of the iterative procedure due to the feedback of modes upon themselves. However, all is not lost; in the next section we suggest a possible solution to the problem.

2.2 Linear difference initialization

Daley and Puri (1980) considered several possible normal mode initialization schemes for use in data assimilation. One of these, suggested on the grounds that it is computationally inexpensive, consisted of a linear normal mode initialization performed on the difference between an analysis and the model-generated field used as first-guess for the analysis. In other words, the analysis scheme is only allowed to change the Rossby modes, and the gravity modes are taken directly from the first-guess. Provided that the first-guess is reasonably accurate, the changes in the Rossby modes should not seriously upset the balance between the nonlinear forcing and the linear time tendencies of the gravity modes. The technique is inexpensive because no iteration is required, nor is it necessary to run the single-timestep model forecast.

The experiments described by Daley and Puri (1980) used a barotropic model, so the question of physical processes did not arise. With a complex model as the vehicle for data assimilation, the "linear difference initialization" technique may produce better results than adiabatic nonlinear normal mode initialization, as well as being more economical.

In order to visualize this statement, we modify the "slow manifold" diagram of Leith (1980). We consider any given state of the model as a point in phase space. The coordinates of the phase space may be gridpoint values of each variable, spectral coefficients, or in this case the coefficients of the Rossby and gravity modes. Schematically we can represent the multi-dimensional phase space on a two-dimensional diagram (Fig.10) with axes R (Rossby modes) and G (gravity modes). If all the gravity mode coefficients are zero, then the state of the model lies on the R-axis; this would be the case after linear normal mode initialization. Nonlinear normal mode initialization is an attempt to balance the linear and nonlinear time tendencies of the gravity modes, in order to remove all high-frequency oscillations; the set of model states in which this has been achieved is called the "slow manifold", indicated by M_A on Fig. 10. If the model is integrated adiabatically from an initial state in M_A, then the subsequent model states will lie in M_A (approximately; here we neglect second-order complications). Initial states outside M_A will lead to integrations oscillating about M_A.

We now recognize that there are actually two slow manifolds to consider: M_A for an adiabatic version of the model, and a different slow manifold M_p for the model with physical processes included.

Let the point A in Fig. 10 represent a particular analysis. L and N represent the same analysis after linear and nonlinear normal mode initialization respectively. Let F represent the first-guess field, which we may (optimistically) assume to be in the slow manifold M_p, since it is model-generated. Then the linear difference initialization technique will take us to the point X, which is closer to the slow manifold M_p than is the point N obtained by adiabatic nonlinear initialization. Of course the diagram has been constructed in such a way as to ensure this result, but it is plausible that the gravity modes from the first-guess field, balanced with respect to physical processes by actually running the model, may be more appropriate than those obtained by nonlinear normal mode initialization, which are correctly balanced with respect to adiabatic nonlinear forcing only.

Returning to the question of the mean meridional circulation, Fig. 11 shows the results after linear difference initialization applied to the analysis of Fig. 8, together with the first guess field of

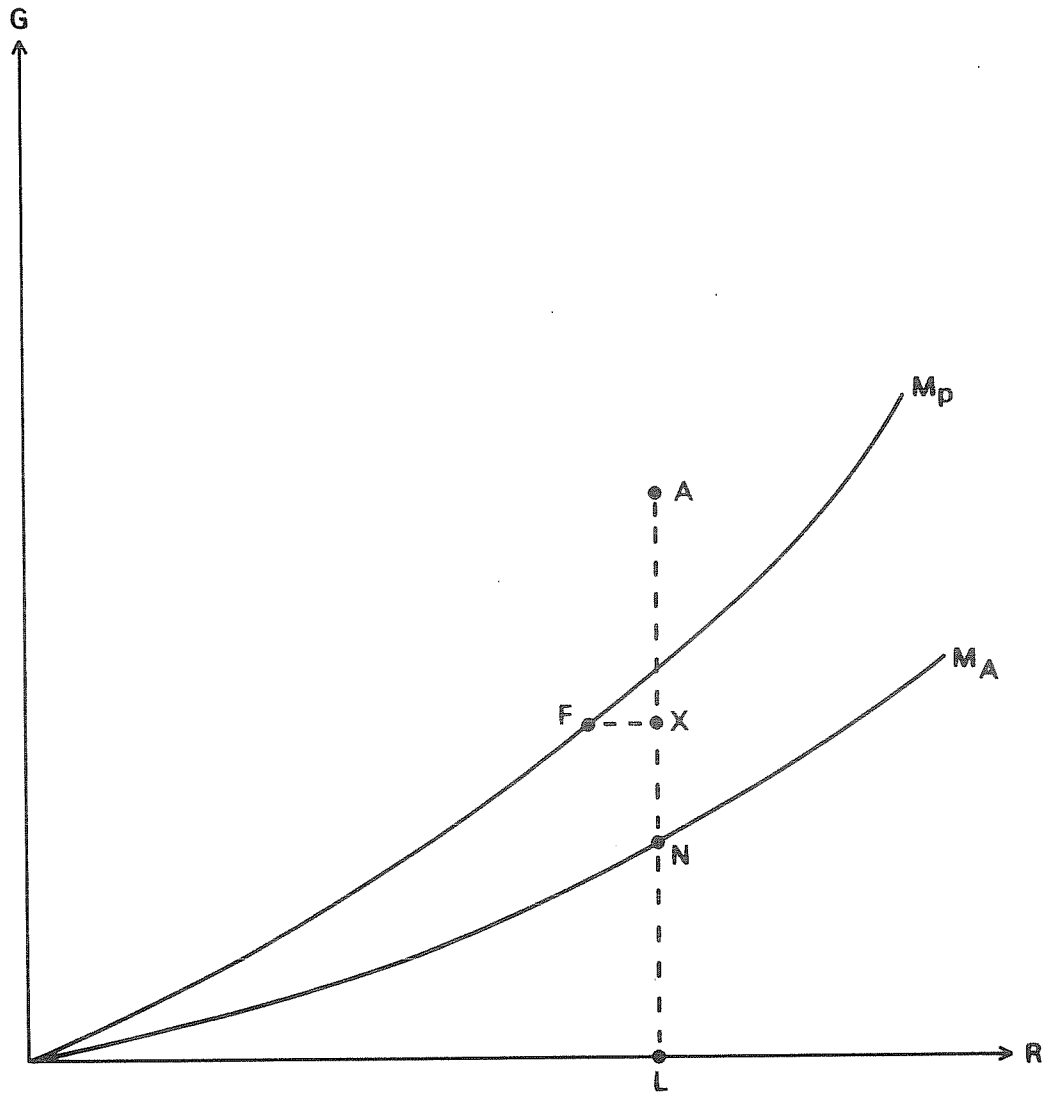

Fig. 10 Representation of initialization techniques on the slow manifold diagram

Fig. 7. Fig. 11 should be compared with Fig. 9 (adiabatic nonlinear normal mode initialization); notice in particular the much better preservation of the Hadley cell. Fig. 12 shows the evolution of surface pressure during 24-hour forecasts with physics from this analysis, before and after linear difference initialization; note that this initialization technique is just as effective in preventing high-frequency oscillations as was nonlinear normal mode initialization.

The only remaining question concerns the stability of the technique in a long data assimilation run. Preliminary results (after a 24-hour five-cycle assimilation experiment) are encouraging, but complete confidence awaits a longer experiment.

2.3 Variational normal mode initialization

One aspect of any initialization technique which we have ignored so far is that it inevitably changes the analysed fields. If the changes are small relative to the expected analysis error, then this is of no importance, but in practice we have found that the changes in the wind field due to normal mode initialization are usually acceptably small, while the changes in the mass field (principally the surface pressure) are rather larger than one would hope. This is simply a consequence of geostrophic adjustment theory, which tells us that for most scales of motion the mass field will adjust to the rotational part of the wind field.

Linear, nonlinear and "linear difference" normal mode initialization methods all change the gravity mode components of the analysed fields, leaving the Rossby modes untouched. The basic idea of variational normal mode initialization (Daley, 1978) is to use these extra degrees of freedom to add a change in the Rossby modes which in some sense compensates for the change in the gravity modes.

Formally, we minimize a variational integral of the form

$$I = \int_0^1 \int_{-\pi/2}^{\pi/2} \int_0^{2\pi} \{\omega_v(\Delta_v)^2 + \omega_h(\Delta_h)^2\} \, d\lambda \, \cos\theta \, d\theta \, d\sigma \qquad (44)$$

subject to the specified changes in the gravity modes. In the definition of I, Δ_v, Δ_h represent changes in the wind field and mass field respectively. ω_v and ω_h are specified weights reflecting our

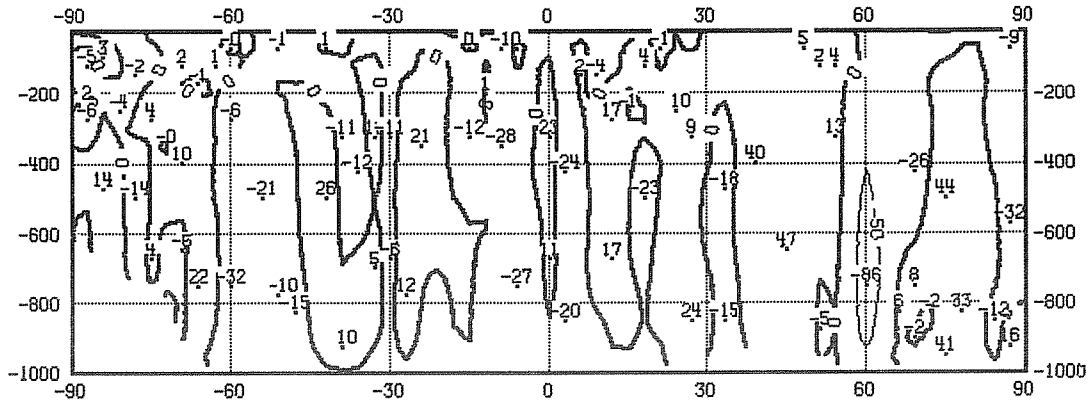

MEAN VERT WIND (DP/DT MPA/S)
1979/ 1/16 0Z IXQ1PA ⊏LINEAR DIFFERENCE⊏ INITIALIZATION

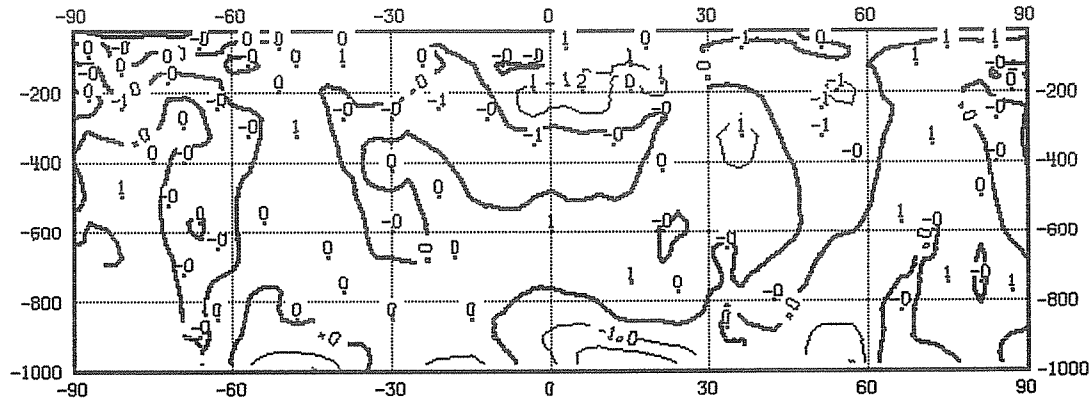

MEAN V-WIND (M/S)
1979/ 1/16 0Z IXQ1PA ⊏LINEAR DIFFERENCE⊏ INITIALIZATION

Fig.11 Mean meridional circulation after "linear difference" initialization

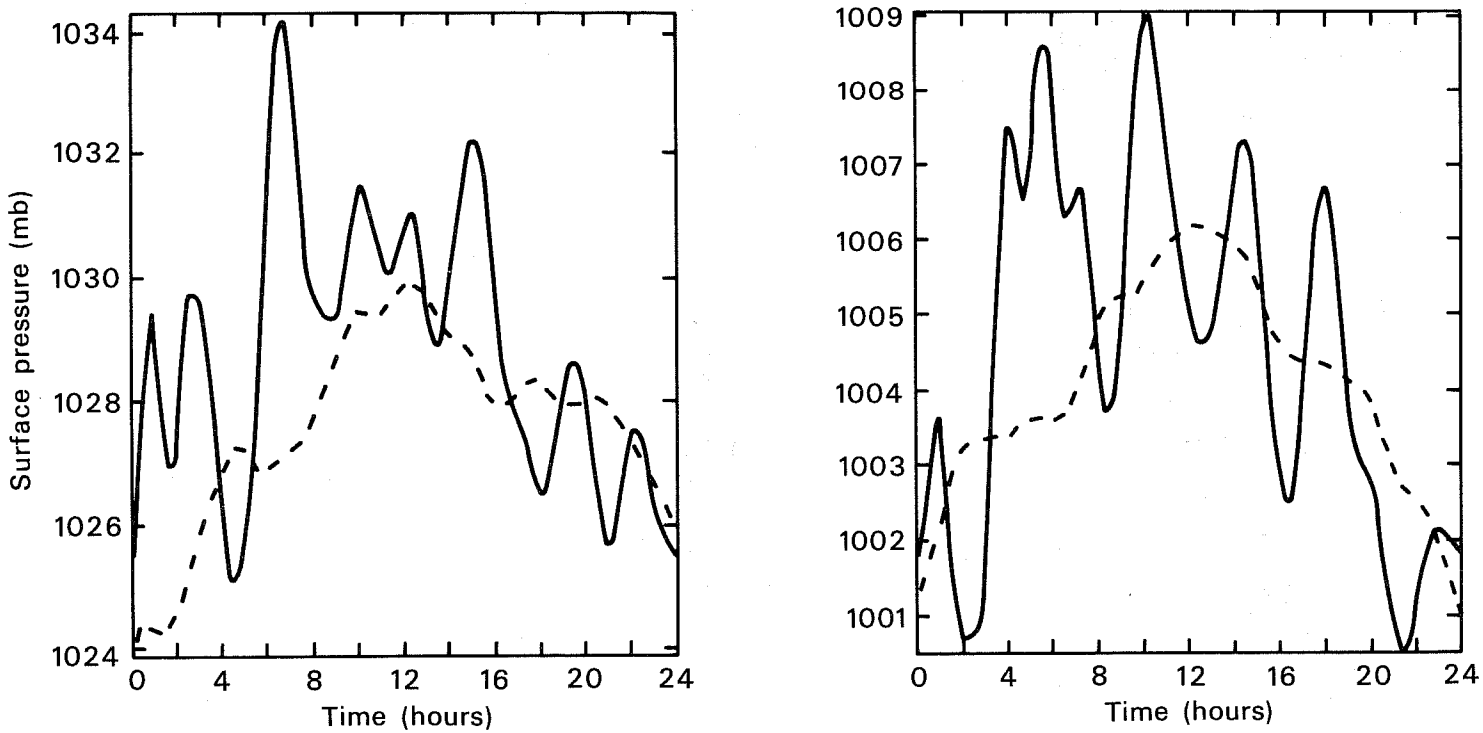

Fig. 12 Surface pressure vs. time at 45°N, 40°W and 40°N, 90°W without initialization (——) and after linear difference initialization (----)

confidence in the analysis of the wind and mass fields. Ideally ω_v and ω_h would be functions of λ, θ and σ, but in order to keep the minimization problem tractable we assume here that they are specified as functions of θ only.

A suitable variational integral for the σ-coordinate model is

$$I = \int_0^1 \int_{-\pi/2}^{\pi/2} \int_0^{2\pi} \{\Phi\omega_v((\Delta u)^2+(\Delta v)^2)+g^2\omega_h(\Delta h)^2\}\, d\lambda \cos\theta\, d\theta\, d\sigma \tag{45}$$

where h is the auxiliary height variable defined by (7), and Φ is an arbitrary geopotential depth included for dimensional consistency. Daley (1978), using a spectral barotropic model, proceeded by using Lagrange multipliers to convert the minimization problem into a set of linear equations for the changes. Here we take a different (but presumably equivalent) approach.

Discretizing in the vertical,

$$I = \sum_{\ell=1}^{L} \left[\int_{-\pi/2}^{\pi/2} \int_0^{2\pi} \{\Phi\omega_v((\Delta u)^2+(\Delta v)^2)+g^2\omega_h(\Delta h)^2\} d\lambda\, \cos\theta\, d\theta \right]_\ell (\Delta\sigma)_\ell \tag{46}$$

To proceed further we assume that we are using normal modes based on an <u>isothermal</u> atmosphere. In this case the vertical normal modes are orthogonal with weight function $(\Delta\sigma)_\ell$, and we can replace Eq. (36) by a sum over vertical normal modes:

$$I = \sum_{m=1}^{L} \left[\int_{-\pi/2}^{\pi/2} \int_0^{2\pi} \{\Phi\omega_v((\Delta\bar{u})^2+(\Delta\bar{v})^2)+g^2\, \omega_h(\Delta\bar{h})^2\} d\lambda\, \cos\theta\, d\theta \right]_m \tag{47}$$

where $\bar{u}$, $\bar{v}$, $\bar{h}$ are defined by (16). Furthermore the orthogonality of the vertical normal modes implies that we can minimize over each vertical mode separately.

Similarly, for each vertical mode m we can discretize along latitude rows and use the orthogonality of the Fourier modes to reduce the problem to one of minimizing an integral of the form

$$I(m,k) = \int_{-\pi/2}^{\pi/2} \{\Phi\ \omega_v((\Delta\tilde{u})^2+(\Delta\tilde{v})^2)+g^2\omega_h(\Delta\tilde{h})^2\}\ \cos\theta\ d\theta \qquad (48)$$

for each zonal wavenumber k, where $\tilde{u}$, $\tilde{v}$, $\tilde{h}$ are defined by (23).

Discretizing (48), using the transformation (28), and treating symmetric and antisymmetric modes separately (again using orthogonality), we find that

$$I(m,k) = \| W^{\frac{1}{2}}\ \Delta\hat{\underset{\sim}{Y}} \|_2 \qquad (49)$$

where $\hat{\underset{\sim}{Y}}$ is the vector containing values of $\hat{u}$, $\hat{v}$, $\hat{h}$ defined in (31), and W is a diagonal matrix containing values of $\Phi\omega_v$ and $(gD_m)\omega_h$ (D_m is the equivalent depth for vertical mode m).

Now, the change in $\hat{\underset{\sim}{Y}}$ due to gravity modes, $(\Delta\hat{\underset{\sim}{Y}})_G$, is specified as a strong constraint. In order to minimize I(m,k) we define a change due to Rossby modes,

$$(\Delta\hat{\underset{\sim}{Y}})_R = E_R\ \Delta\underset{\sim}{c}_R \qquad (50)$$

where E_R is a matrix whose columns are the Rossby mode eigenvectors, and $\Delta\underset{\sim}{c}_R$ is a vector of (unknown) changes to the Rossby mode coefficients. Since $(\Delta\hat{\underset{\sim}{Y}}) = (\Delta\hat{\underset{\sim}{Y}})_G + (\Delta\hat{\underset{\sim}{Y}})_R$, the problem of minimizing I(m,k) reduces to solving the linear least-squares problem

$$W^{\frac{1}{2}}\ E_R\ \Delta\underset{\sim}{c}_R = -\ W^{\frac{1}{2}}\ (\Delta\hat{\underset{\sim}{Y}})_G \qquad (51)$$

The whole procedure can conveniently be interpreted on the "slow manifold" diagram, see Fig.13. Changing the gravity mode coefficients (e.g. by the usual nonlinear correction procedure) takes us from the analysis point A to the point N, on or near the slow manifold. Changing the Rossby mode coefficients by solving Eq. (51) takes us along a line parallel to the R-axis, until a minimum value of the variational integral I is found, at point M. The procedure can of course be iterated; it is then convenient, as in Daley (1978), to define I in terms of changes over each iteration rather than over the whole procedure.

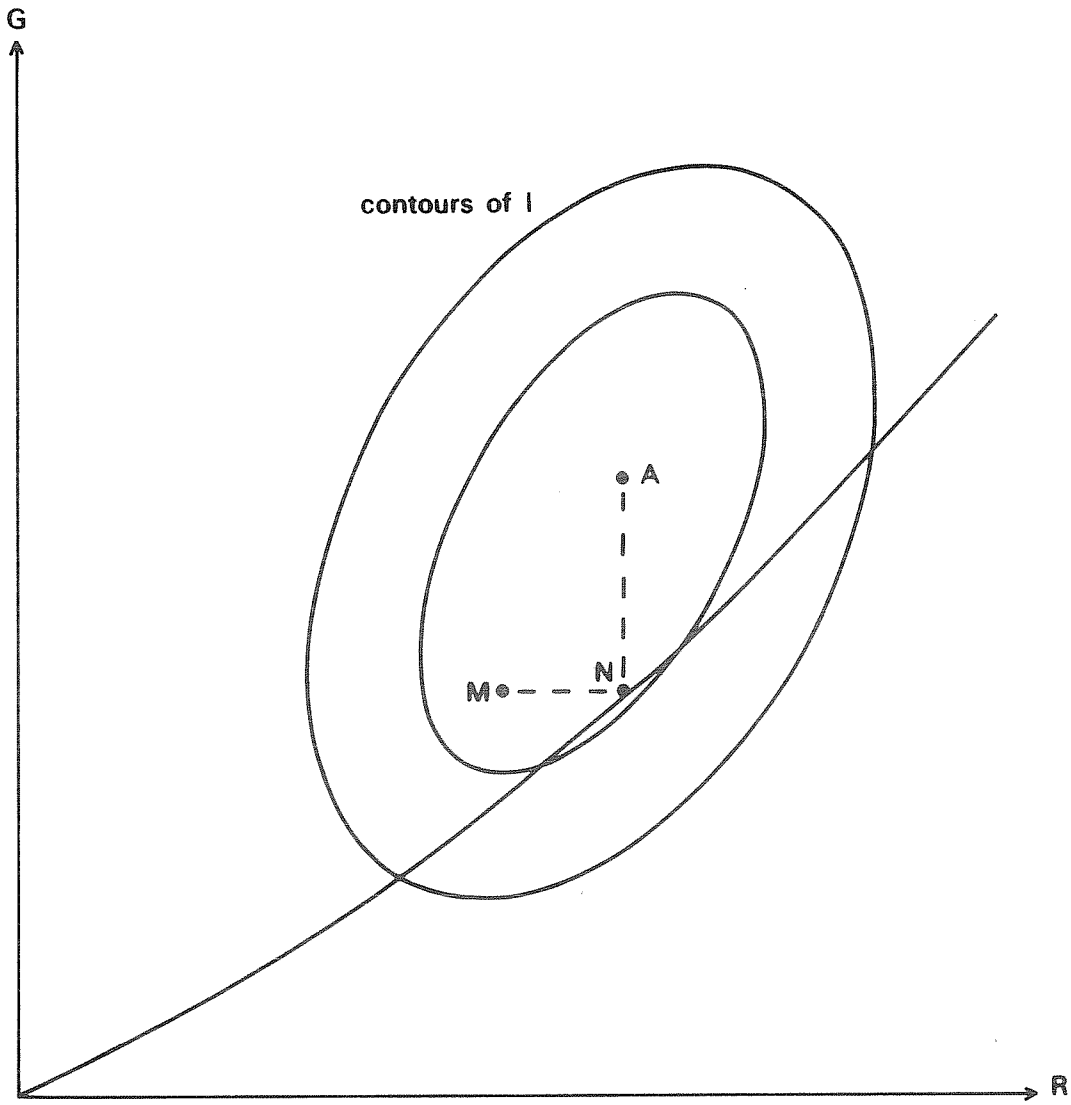

Fig.13 Variational initialization on the slow manifold diagram

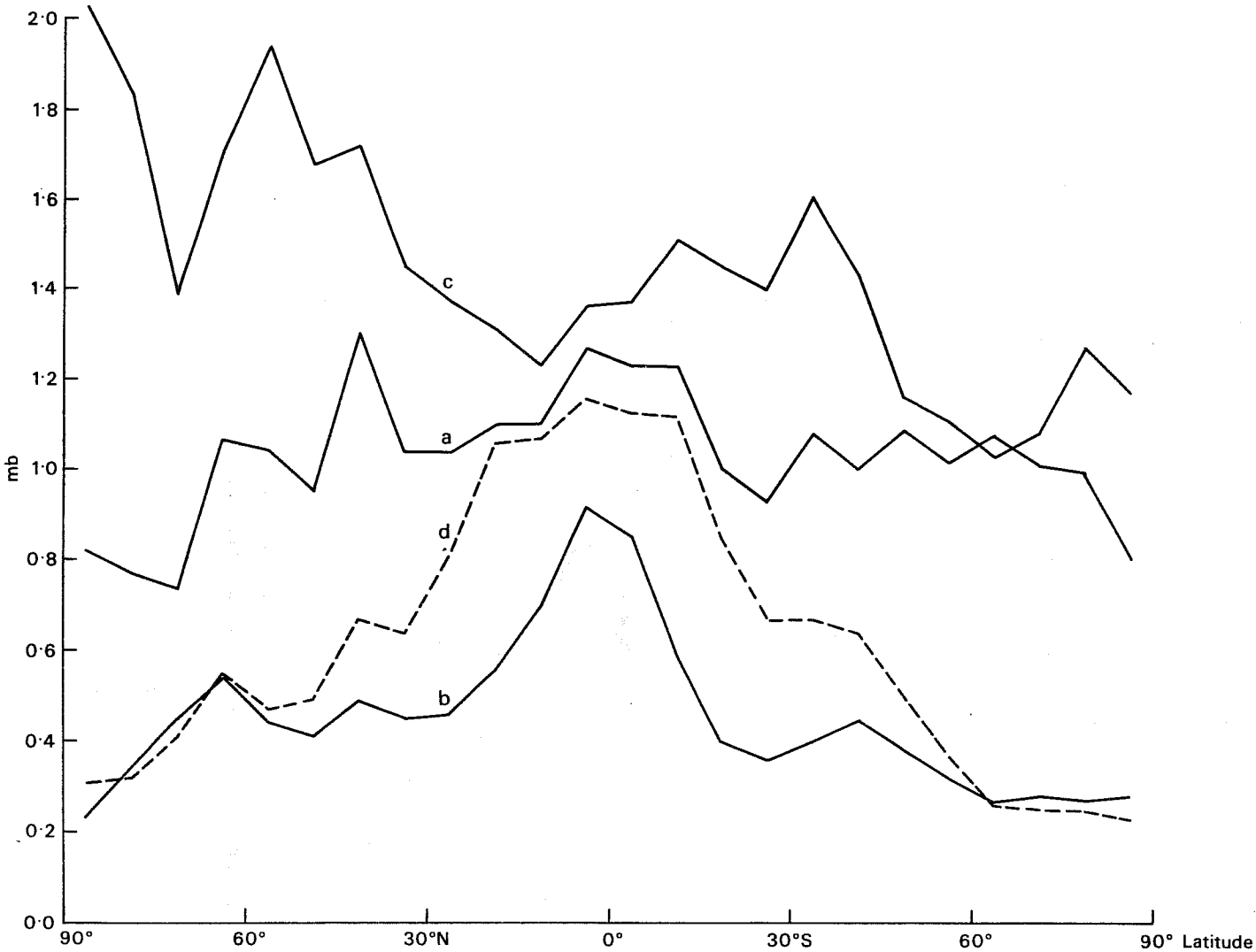

Fig. 14 Rms changes in surface pressure (vs. latitude) :

(a) standard initialization

(b) variational; $\omega_v=0$, $\omega_h=1$

(c) variational; $\omega_v=1$, $\omega_h=0$

(d) variational; $\omega_v=0.04\ \cos^4\theta$, $\omega_h=1-\omega_v$

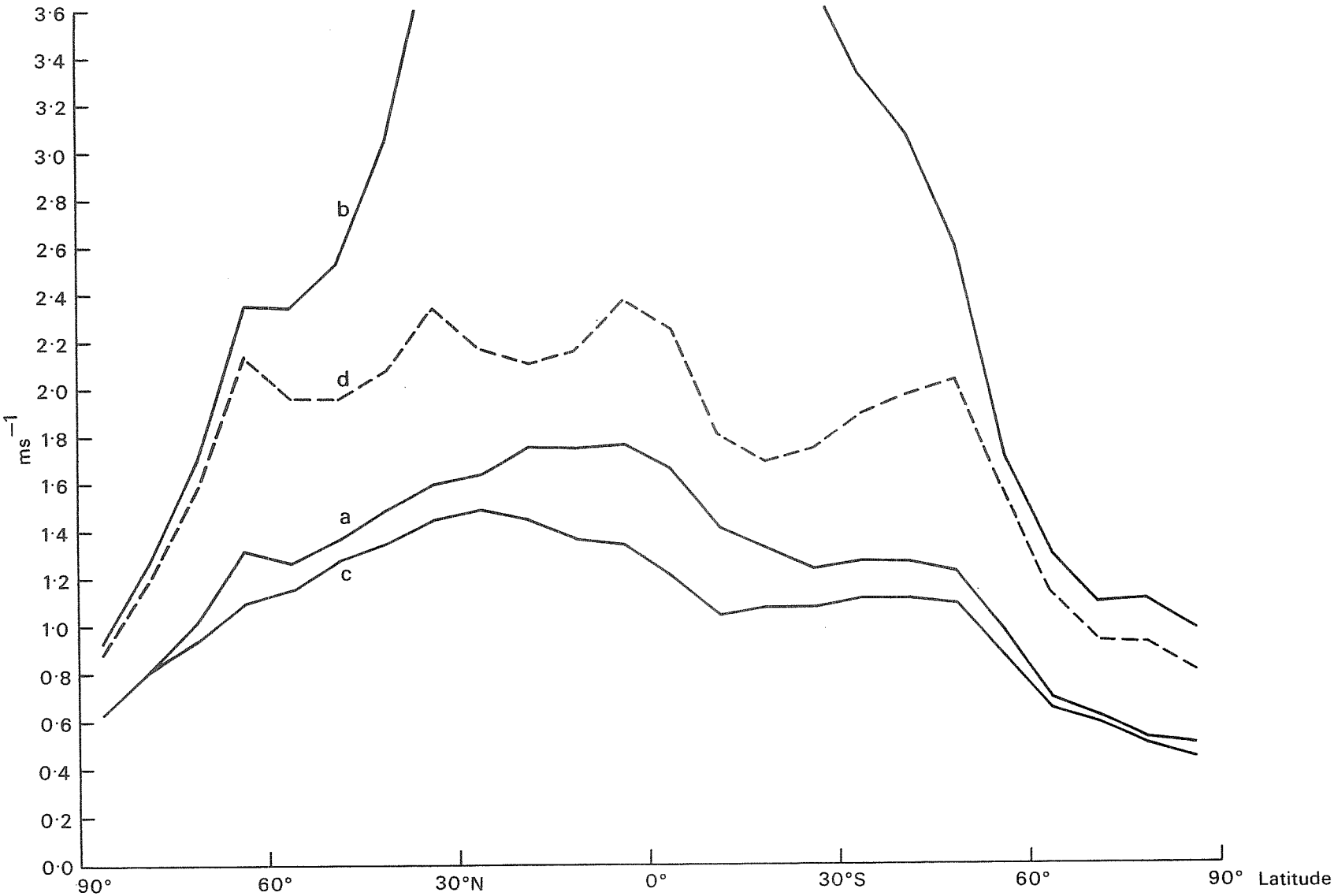

Fig. 15 As Fig. 14, but for rms wind changes

It remains to determine suitable functions ω_v, ω_h. Some results are presented in Figs. 14 and 15, which show the root mean square changes in p_s and vector wind $\underline{V}$ as functions of latitude. Setting $\omega_v = o$, $\omega_h = 1$ in an attempt to minimize the changes in the mass field results in catastrophic changes in the tropical wind field. Setting $\omega_v=1$, $\omega_h=o$ results in large (but not so drastic) changes in the surface pressure field. Setting $\Phi = gD_1$, $\omega_v = 0.04 \cos^4\theta$, $\omega_h = 1 - \omega_v$ produces more reasonable results. It should be mentioned that, recognizing that most of the changes take place on medium and large horizontal scales, the minimization was only performed for zonal wavenumbers $o \leqslant k \leqslant 15$, and only 15 latitudinal Rossby modes were used for each (m,k). Extending the truncation might further improve the results. Finally, test integrations confirm that variationally initialized data sets still yield forecasts almost completely free of high-frequency oscillations.

References

Andersen, J.H. 1977 A routine for normal mode initialization with non-linear correction for a multi-level spectral model with triangular truncation, ECMWF Internal Report No.15.

Burridge, D.M. and Haseler, J. 1977 A model for medium range weather forecasting - adiabatic formulation. ECMWF Technical Report No. 4.

Daley, R. 1978 Variational non-linear normal mode initialization. Tellus, 30, 201-218.

Daley, R. and Puri, K. 1980 Four-dimensional data assimilation and the slow manifold. Mon.Wea.Rev., 108, 85-99.

Dickinson, R.E. and Williamson, D.L. 1972 Free oscillations of a discrete stratified fluid with application to numerical weather prediction. J.Atmos.Sci., 29, 623-640.

Leith, C.E. 1980 Nonlinear normal mode initialization and quasi-geostrophic theory. J.Atmos.Sci., 37, 958-968.

Longuet-Higgins, M.S. 1968 The eigenfunctions of Laplace's tidal equations over a sphere. Phil.Trans.Roy.Soc.London, A262 511-607.

Machenhauer, B. 1977 On the dynamics of gravity oscillations in a shallow water model, with application to normal mode initialization. Contrib.Atmos.Phys., 50, 253-271.

Nitta, T. 1969 Initialization and analysis for the primitive equation model. Proc. WMO/IUGG Symposium on Numerical Weather Prediction, Tokyo, Japan, 26 Nov - 4 Dec 1968, pp. VI, 11-20, Japan Meteorological Agency, Tokyo, 1969.

Temperton, C. 1977 Normal modes of a barotropic version of the ECMWF gridpoint model. ECMWF Internal Report No.12.

Temperton, C. and Williamson, D.L. 1979 Normal mode initialization for a multi-level gridpoint model. ECMWF Technical Report No. 11.

Williamson, D.L. 1976 Normal mode initialization procedure applied to forecasts with the global shallow water equations. Mon.Wea.Rev., 104, 195-206.

Williamson, D.L. and Dickinson, R.E. 1976 Free oscillations of the NCAR global circulation model. Mon.Wea.Rev., 104, 1372-1391.